Proceedings of the Institution of Civil Engineers
Engineering and Computational Mechanics 162
March 2009 Issue EM1
Pages 3–9
doi: 10.1680/eacm.2009.162.1.3
EACM 700014
Received 15/12/2007
Accepted 29/09/2008
Keywords: concrete structures/failures/strength and testing of materials

John N. Karadelis
Senior Lecturer, Department of Civil Engineering, Coventry University, UK

ice
Institution of Civil Engineers

Concrete grandstands. Part I: experimental investigation

J. N. Karadelis MPhil(Eng), TEE

Loading–unloading tests were carried out on uncracked (as delivered from the factory) and cracked (after the first loading–unloading cycle was completed) grandstand terrace units. The variation of parameters, such as displacements and strains, with the applied load was recorded and presented in a graphical form. The reduction in stiffness of the units owing to cracks was estimated from these graphs. The predominant mode of failure was found to be cracking initiated at the soffit of the units (tension zone) and mainly around the symmetry line (where maximum bending stresses congregate). These cracks propagated gradually towards the top. The measured and predicted strain distribution across the depth of the vertical part of the terrace unit (riser) was found to be predominantly linear, displaying tension at the bottom and compression at the top. A large portion of the horizontal part of the unit (tread) followed closely the behaviour of the riser, however, to reveal tension rather than compression at the top. This could have some implications for the design of the units. It was concluded that present methods and procedures of evaluating and designing precast concrete terrace units are not integral. Further tests are required, coupled with more analytical work. A Part II companion paper reports on the development of a numeric algorithm describing the analysis process.

NOTATION

F load
k stiffness
δ displacement

1. INTRODUCTION

The most common construction of sports stadia today is that of a hybrid type where precast concrete terrace units span between inclined (raker) steel beams and rest on each other, thus forming a grandstand (Figure 1). The role of the third (resting) support is to stop the units from undergoing excessive twisting and, in general, provide extra stability. Accurate analysis and optimum design of these prefabricated units (elements), as well as the grandstand as a whole, requires a good understanding of their behaviour and performance under static and dynamic loading. Optimising their structural sections and improving economy, safety and comfort in use, is an ongoing engineering challenge with industry and academia working in tandem.

In particular, the applied loads and load mechanisms generated by sports and music fans on grandstand and other stadium structures are not yet fully understood or benchmarked. Codes of practice in the UK and abroad are not as rigorous and informative as they should be. Understanding the influence of these loads on grandstands would necessitate short- and long-term investigations on suitable structures. Their mathematical 'reproduction' would require complex numerical techniques, based on and supported by experimental findings.[1]

The current paper is part of an ongoing research programme at Coventry University, aiming to extend the understanding of the structural behaviour of sports stadia assembled from interconnected precast concrete units, by providing all those interested with a rigorous interpretation (numerical modelling) of the behaviour of these structures, initially under static loads (published as a seperate part II paper)[2] and later under dynamic actions.

2. EXPERIMENTAL PROGRAMME, METHODOLOGY AND PROCEDURES

A series of comprehensive laboratory tests were carefully planned and executed. The aim of this preliminary investigation was twofold. First, to examine the behaviour of a family of reinforced concrete (RC) structures supported at three positions and undergoing static, incremental loading. Second, to estimate the uncracked and fully cracked stiffness of the units. Two tests per unit were carried out for the latter. Test 1 assumed the section uncracked, as it was delivered from the factory; test 2 considered the same section, this time fully cracked, as received from test 1. Three 'identical' units made of

Figure 1. A precast concrete grandstand

the same batch were tested to failure. The vast majority of the data collected, correlated well. For reasons of clarity, only the results from unit 1 will be reported here.

The L-section terrace units were designed, manufactured and transported to Coventry University. Owing to limited space in the laboratory the smallest actual size was ordered. They were approximately 4·8 m long, encompassing a 700 mm wide by 100 mm thick horizontal member (tread) and 150 × 275 mm upstand (riser), as per Figure 2. Their properties are shown in Table 1.

The design was based on BS 8110[3] and produced the results shown in Tables 2 and 3. It is clear from these tables that, for design purposes, the units were considered simply supported at the ends only and analysed as spanning the long dimension. Constructional details show the units spanning between two steel raker beams with two steel 'stools' welded on the rakers providing the necessary platform under the riser. Each unit is propped along the front edge by the riser of the lower unit.

The raker beams were not reproduced in the laboratory for obvious reasons. Instead, two steel 'stools' were placed under the riser, spanning 4·5 m apart. A suitable UB-section was placed under the front edge imitating the riser of the lower unit on site. Elastomeric bearings (neoprene pads) were inserted between the two materials as per actual conditions.

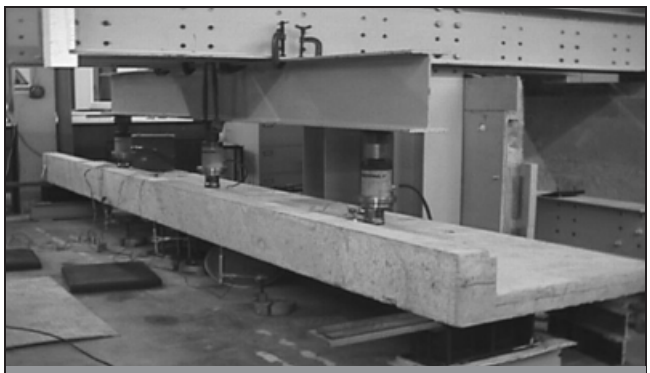

Figure 2. A precast concrete terrace unit as set up for testing in the laboratory

Material properties	Loading	Cover to reinforcement
Characteristic concrete strength, f_{cu} = 45 N/mm^2	Load type: Uniformly distributed load	30 mm at sofit and the sides of riser and 40 mm at the top of tread
Reinforcement (T&C) characteristic strength, f_y = 460 N/mm^2	Dead load (self-weight) = 3·650 kN/m^2	
Reinforcement (shear) characteristic strength f_{yv} = 460 N/mm^2	Imposed load = 4·000 kN/m^2	

Table 1. Material properties, loading and cover to reinforcement

Serviceability state	Ultimate limit state
Reactions: $R_1 = R_2$ = 12·056 kN Maximum bending moment = 13·563 kN m @ mid-span	Reactions $R_1 = R_2$ = 18·139 kN Maximum bending moment = 20·406 kN m.@ mid-span

Table 2. Forces and moments

Effective depth, d = 230 mm
K-factor = 0·091
Lever arm factor = 0·886
Lever arm, z = 205·8·8 mm
Depth to neutral axis, s = 76·6 mm
Area of tension steel required, A_{st} = 258 mm^2
Tension steel provided = 1T20 (314 mm^2)
Area of compression steel required, A_{sc} = 0 mm^2
Compression steel provided = 1T12 (113 mm^2)

Table 3. Output details

The heavy structures area of the civil engineering laboratories, comprising a strong floor and an array of rearrangeable steel stanchions and beams, was utilised. Six concentrated loads, which were equal in magnitude, simulated a uniformly distributed load (UDL) and were applied on the tread at 700 mm centres (Figure 2), using hydraulic jacks and spreader beams. The line of action of the UDL was parallel to the riser and at a clear distance of 100 mm from it. The load was applied incrementally and was kept constant during the collection of data. Loading and unloading tests were performed for 'uncracked' and 'fully cracked' units. The following parameters (variables) were measured using a series of appropriate transducers shown schematically in Figure 3.

(*a*) The maximum displacement was measured at the centre of the unit, under the riser and at two other symmetrical positions, to ensure symmetrical behaviour.
(*b*) The surface strain of the longitudinal tension (bottom) reinforcement of the riser, using electrical resistance strain gauges (ERSGs).
(*c*) Also, ERSGs were used to measure the strain at the lateral bottom reinforcement of the riser/tread.
(*d*) The concrete surface strain distribution across the depth of the riser section, using four pairs of demec points.
(*e*) The concrete surface strain at seven other positions on the unit, using demec points and a set of mechanical (analogue) strain gauge dials.

It was envisaged that the above measurements should provide a good understanding of the behaviour of the terrace unit.

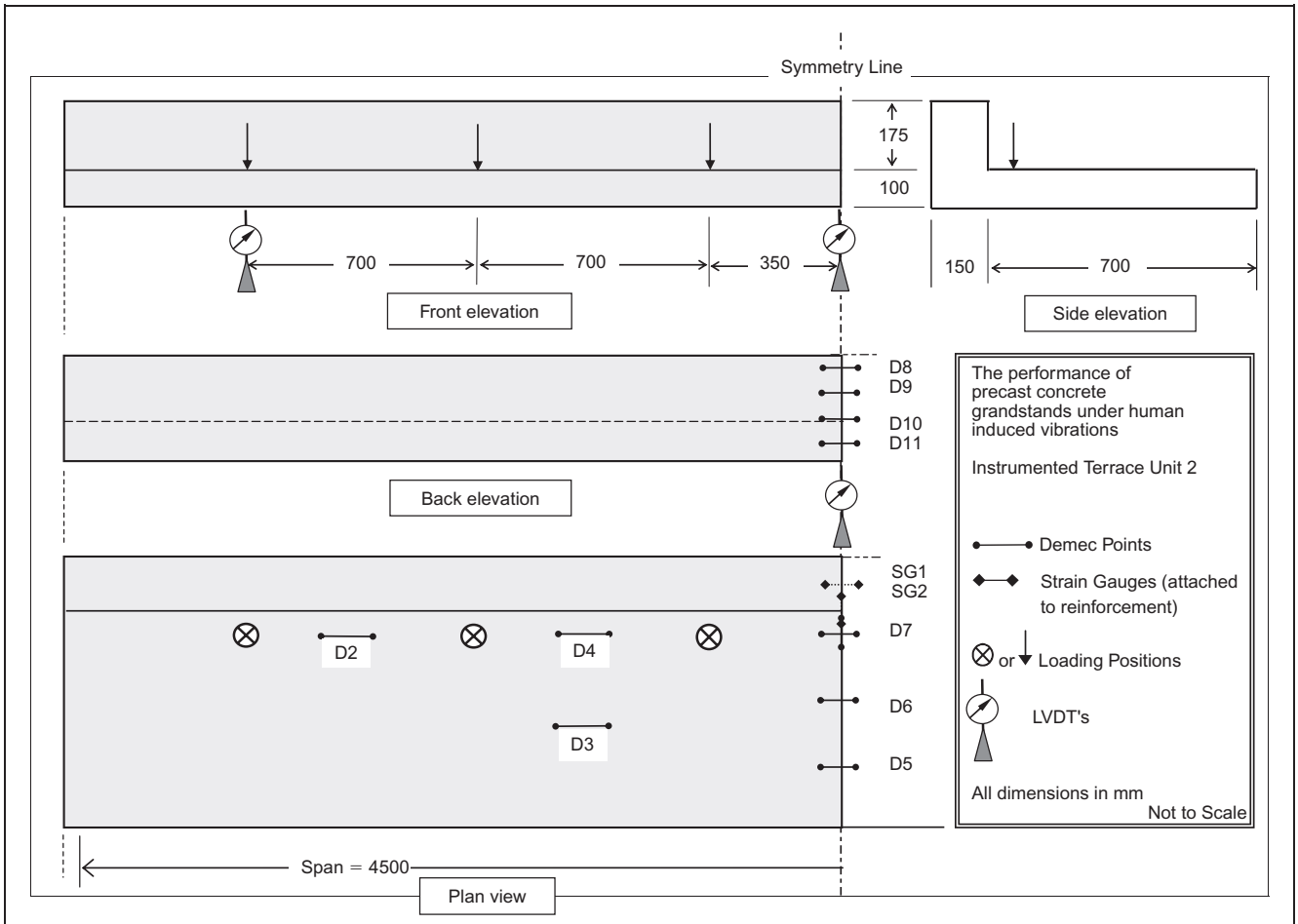

Figure 3. Terrace units 1 and 2, main reinforcement and instrumentation layout

3. RESULTS AND DISCUSSION

3.1. Displacements

Figure 4 shows loading and unloading paths of maximum displacement measured at mid-span using linear variable differential transducer, (LVDT 2) for uncracked and fully cracked units. The same figure, showing the performance of the units in terms of their deflection, can be used as an index of their conformity. Tests 1 and 2, 3 and 4, and 5 and 6 refer to units 1, 2 and 3 respectively. Odd numbers denote tests on uncracked units.

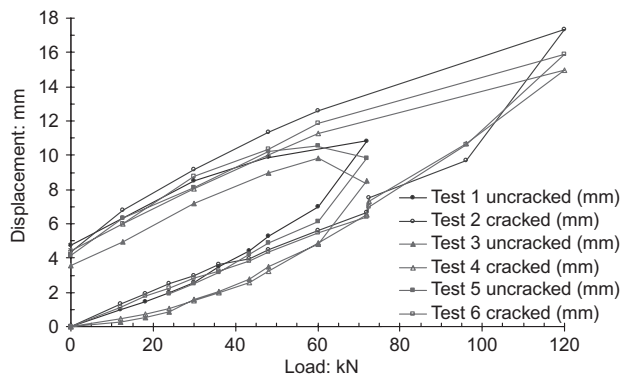

Figure 4. Terrace units 1, 2, 3. Tests 1 and 2 (uncracked and fully cracked units). Comparison between maximum displacements (LVDT2). Loading–unloading

Units 1 and 3 are in good agreement while unit 2 shows a little variation. Table 4 summarises and presents the above in terms of their percentage difference. All differences were based on deflection values related to maximum loads reached—that is, 72 kN for the uncracked and 120 kN for the cracked units.

It is evident that the path described by curve test 2 is smoother and not characterised by any sudden 'strain jumps', until after it exceeds the maximum value of 72 kN met in test 1. Beyond this load further cracking takes place, producing another 'strain jump' and permanent deformation.

Up to a load of 30, possibly 32 kN, all slopes are similar, approximating linear behaviour and showing good correlation. This compares well with the ultimate design load of 36 kN allowed by the designer. After the first initial cracking in test 1 (above 30 kN), however, the two curves diverge. The displacement of the uncracked section becomes noticeably higher compared to that of the cracked. At 60 kN the corresponding displacements for the uncracked and cracked sections were 6·98 and 5·6 mm respectively. At 72 kN (the maximum load allowed for the uncracked unit) the corresponding displacements were 10·75 mm and 6·5 mm.

Considering that the fully cracked unit has suffered some permanent deformation owing to loading at test 1, it is not surprising that its displacement values are now lower than those of the uncracked section. The maximum displacement

Uncracked units		Cracked units	
Test X and test Y	Percentage difference	Test X and test Y	and age difference
1 + 3	18·0	2 + 4	13·2
1 + 5	9·2	2 + 6	8·0
3 + 5	10·7	4 + 6	5·6

Table 4. Percentage difference in terms of deflection between units 1, 2 and 3

reached by the cracked unit was 17·25 mm at 120 kN. The permanent displacement after load removal was found to be approximately 4·5 mm in both tests.

Adding residual displacements to test 2, inherited from test 1, would yield

Total displacement at test 2 =

4·5 mm + 6·5 mm = 11·00 mm @ 72 kN

This is only marginally higher than the corresponding displacement of 10·75 mm of test 1 and could demonstrate (along with the statement that both tests gave similar residual displacements) a similar behaviour of the unit before and after cracking.

3.2. Strain distribution across the depth of the riser

Figures 5 and 6 show the distribution of strain per load increment for an initially uncracked (test 1) and a cracked (test 2), section respectively. Strain was measured across the vertical symmetry line and at four different levels above the soffit of the riser (D11 = 40 mm, D10 = 110 mm, D9 = 165 mm and D8 = 235 mm).

The strain diagram in Figure 5 shows perfectly linear behaviour up to and including the load increment of 30 kN. This is compatible with the findings shown in Figure 4. The applied load was resisted by both concrete and reinforcement. Tension is gradually transferred to the reinforcement as the first cracks at the bottom of the unit appear, characterised by a nonlinear distribution of strain for load increments of 48, 60 and 72 kN. Equilibrium of the section is maintained by a gradual movement upwards of the neutral axis, reducing the area of section in compression. Figure 6 presents a similar account; this time the strain was distributed more smoothly. Once the cracks are developed, no sudden changes of strain are present during reloading. These cracks open wider following load increments, while strain readings reach higher values.

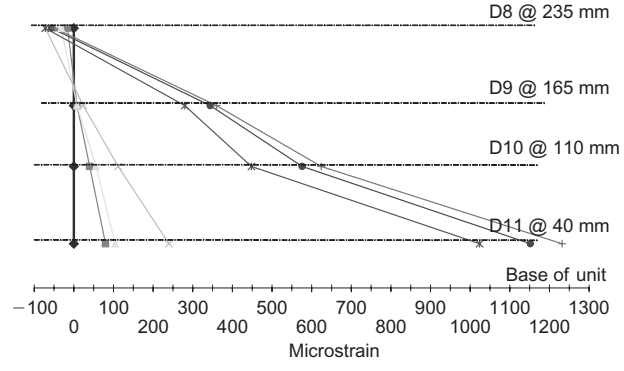

Figure 5. Terrace unit 1, test 1, strain distribution per load increment across the depth of the riser

3.3. Strain measured at the reinforcement

Electrical resistance strain gauges were attached to the reinforcement as shown in Figure 3. SG1 was attached to the transverse reinforcement and SG2 to the longitudinal tension reinforcement of the riser. Their variation with load increments is shown in Figure 7. As expected, readings of strain gauge SG2 were found to be significantly higher than those of SG1, indicating that main bending took place in the longitudinal direction. Once again, the 30 kN and 48 kN loads were characterised by sudden strain jumps and possible local de-bonding. Maximum values recorded were: $SG1_{max} = 110\ \mu\varepsilon$ and $SG2_{max} = 2100\ \mu\varepsilon$ corresponding to magnitudes of stress of 22 N/mm^2 and 420 N/mm^2 respectively, assuming a modulus of elasticity for steel, $E_{steel} = 200$ kN/mm^2 and a linear stress–strain relationship.

The strain curves for test 2 (cracked section) are a good deal smoother than those of test 1. Strain gauge SG1 showed no strain up to a load of 60 kN. It recorded a strain of 100 $\mu\varepsilon$ for

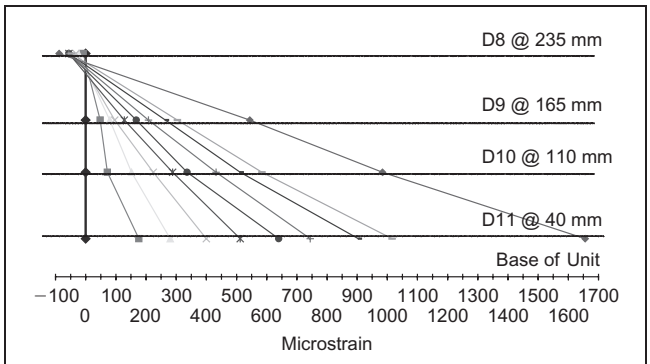

Figure 6. Terrace unit 1, test 2, strain distribution per load increment across the depth of the riser

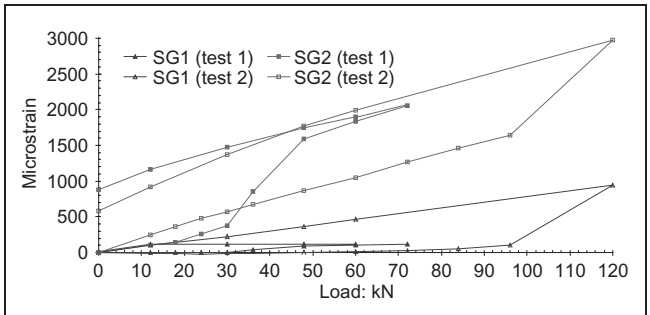

Figure 7. Terrace unit 1, tests 1 and 2, comparison between strains SG1 and SG2, loading–unloading

96 kN and a 'strain jump' to 900 με (180 N/mm^2) for the final load of 120 kN. No residual strain was noticed after unloading, indicating that any cracks formed across the transverse reinforcement must have gradually closed during the unloading procedure. SG2, attached to the main tension reinforcement of the riser, showed a near linear behaviour reaching 1600 με (320 N/mm^2) for 96 kN, before it finally reaches 3000 με (600 N/mm^2, well beyond the yield stress of steel) for 120 kN.

3.4. Strain at SG1, D1, D3 and D4

Figure 8 shows very similar strain patterns for demec pairs D1, D3 and D4, as expected, confirming the validity and accuracy of the readings obtained. D1 reached a maximum and levelled at −500 με, D3 at −250 με and D4 hovered around zero. There was a noticeable gradual reduction in lateral compressive strain from the extreme support regions to the symmetry line. This indicated an independent behaviour of the tread near the supports and a similar one to the riser near mid-span. That is, although the tread, as a structural section itself, developed compression and tension at top and bottom faces near the supports, the entire section was below the neutral axis of the riser (and therefore in tension) near the centre.

Based on Table 2, the total serviceability and ultimate state loads were 24·1 kN and 36·3 kN respectively. The longitudinal strain, measured at D7 and D6, turned tensile at 24 kN and 30 kN respectively (Figure 9). Also, the lateral strain at D4 turned tensile at 30 kN (Figure 8). This would indicate that when the unit is about to reach its allowable serviceability

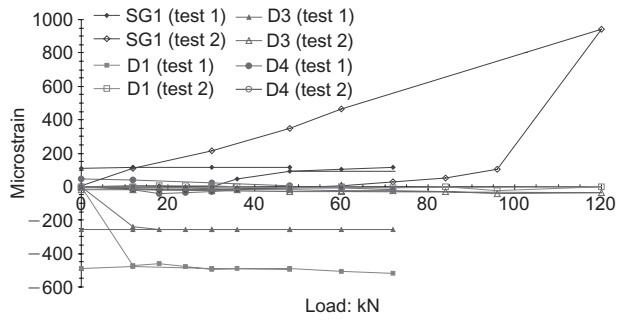

Figure 8. Terrace unit 1, tests 1 and 2, comparison between strains SG1, D1, D3, D4, loading–unloading

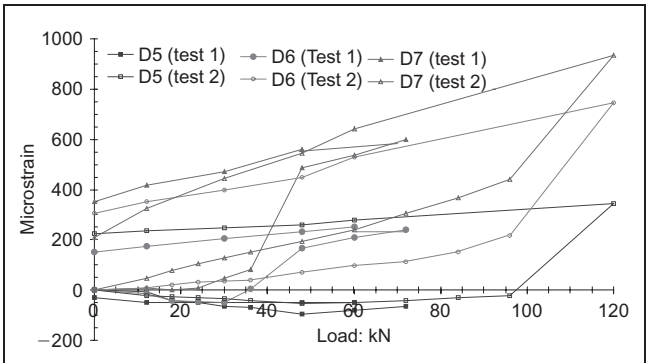

Figure 9. Terrace unit 1, tests 1 and 2, comparison between strains D5, D6, D7, loading–unloading

load, part of it does not obey classical RC theory as tension develops on the top surface. This has not been taken into account when designing the terrace units. The sensitivity of all three demec pairs was greatly reduced at test 2, resulting in strain readings very close to zero. It is envisaged that this was due to the development of a series of cracks outside the effective zone of the demec pairs. SG1, the strain gauge attached to the lateral bottom reinforcement of the tread, recorded tension in both tests. It is clear from Figure 8 that the top of the tread develops cracks at 12 kN (plain concrete), whereas the bottom develops its first cracks at 30 kN (composite action). It is important to remember that the top of the tread near the centre behaves in a different manner, with the whole (tread) section being in tension, following the behaviour of the riser. Yet, for cracking in the same direction, the bottom face will still crack under tension before the top face.

3.5. Strain at D5, D6 and D7

Demec point pairs D5, D6 and D7 were placed at mid-span measuring longitudinal strain as shown in Figure 3. Figure 9 shows the variation of strain with load as measured across these points. It is interesting to note that D5 has followed a compressive path, reaching strain of −100 με at 48 kN and then somehow 'softening', to finish with −70 με at the maximum load of 72 kN allowed for test 1.

In contrast, D6 and D7 have recorded considerably larger tensile strains. Tension in this region is somehow surprising, especially when this is developing along the span of the unit. It shows that the tread at the region identified between the riser and demec points D2 and D5 (Figure 3) follows the behaviour of the riser; that is, it is in tension and forms a 'trough'. The familiar pattern at 12 kN and 30 kN, discussed previously, is repeated here. There is, however, an enormous strain jump between load increments of 30 kN and 50 kN. This is more obvious from demec readings D6 and D7. As strain is recorded tensile, it confirms that concrete has yielded locally.

The loading and unloading paths during test 2 (fully cracked unit) were much smoother than the corresponding in test 1. D5 (Figure 9) showed a negative initial tendency with most of the readings appearing below the horizontal axis. This was also the norm of the corresponding demec pair for the uncracked unit in test 1. New cracks, or further opening of the existing cracks, appeared at 96 kN. The final strain values at 120 kN reached 350, 725 and 925 microstrain for D5, D6 and D7 respectively, whereas residual strains were 225, 300 and 200 microstrain for the same transducers.

3.6. Strains at SG2 and D11

Figure 10 shows a comparison between strains measured by strain gauge SG2, attached to the tension reinforcement of the riser and demec points D11, attached 40 mm above the bottom of the same riser. That is, both SG2 and D11 were at approximately the same level from the soffit of the riser. Initially, and up to the load of 18 kN, both strains showed good correlation, turning reasonably good up to 30 kN. Beyond the branded 30 kN load, however, SG2 produced considerably higher strain values than D11, although both strain paths were remarkably similar. This would indicate the beginning of failure for the surrounding concrete. Also, as new cracks

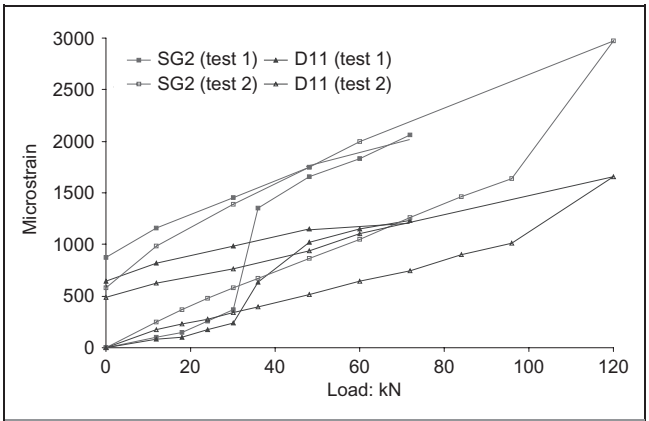

Figure 10. Terrace unit 1, tests 1 and 2, comparison between strains SG2 and D11, loading–unloading

develop in the vicinity, the crack captured by D11 has now ceased opening.

Maximum values of strain recorded for the final load of 72 kN were 2100 $\mu\boldsymbol{\varepsilon}$ and 1200 $\mu\boldsymbol{\varepsilon}$ for SG2 and D11 respectively.

There is as yet no standard test for directly determining the tensile strength of concrete; the latter can be taken as approximately equal to 1/10 of its compressive strength. Hence, in the absence of more scientifically based research, the modulus of elasticity of concrete in tension was taken as equal to 1/10 of that in compression. This allowed for the evaluation of the corresponding stresses for SG2 and D11, as 420 N/mm^2 and 3·6 N/mm^2 respectively. The latter should, however, be regarded with extreme caution.

The unloading procedure was carried out without surprises giving residual strain values of 880 $\mu\boldsymbol{\varepsilon}$ and 640 $\mu\boldsymbol{\varepsilon}$ for SG2 and D11 respectively.

The behaviour of the curve in test 2 was smoother and more linear compared with that of test 1. Although both strain paths are similar, SG2 produced higher strain values for reasons already explained above. Maximum strain was reached at 120 kN, with magnitudes equal to 3000 $\mu\boldsymbol{\varepsilon}$ (600 N/mm^2) and 1650 $\mu\boldsymbol{\varepsilon}$ (49·5 N/mm^2), for SG2 and D11 respectively. Both stress values were well beyond the yield stress values of the materials. Finally, unloading produced residual strains of 600 $\mu\boldsymbol{\varepsilon}$ and 500 $\mu\boldsymbol{\varepsilon}$ for SG2 and D11 respectively.

4. EVALUATION OF STIFFNESS

Static stiffness was estimated from the displacement–load graph in Figure 4. It was not possible to obtain a unique stiffness value as the slope of the $\boldsymbol{F}$–δ curve changed each time a new crack appeared on the unit. The domain of $\boldsymbol{F}$–δ curve of unit 1 was therefore divided into six convenient sub-domains and the 'best-fit' straight line was fitted in each one. The stiffness (slope) of the line was calculated based on the relationship

$$\boldsymbol{F} = k\delta \quad \Rightarrow \quad k = \boldsymbol{F}/\delta \tag{1}$$

The magnitude of these 'local stiffnesses' along with their difference—that is, uncracked minus cracked local stiffness (test 1-2)—are shown in Figures 11 and 12. It is apparent that when a new crack appeared on the unit, its stiffness was reduced. It is also clear that although stiffness values extracted from the uncracked unit were higher than those of the cracked, the former were not, in general, significantly higher. Also, the difference between the two reduced with increasing load, in some way highlighting the importance of steel reinforcement and the concept of ductility.

5. CONCLUSIONS

The following are evident from the incremental, static, loading–unloading tests, carried out on two precast concrete terrace units under laboratory conditions.

(*a*) The predominant mode of failure is the appearance of hair-like cracks at the soffit of the units and around the symmetry line (where bending stresses are maximum) and their gradual propagation upwards.

(*b*) The units are supported at the ends (under the riser) and propped along the front edge of the tread. Hence, they experience a combined bending and (to a lesser extent) torsional effect when loaded near the riser side. This has a knock-on effect on the deformed shape of the units, which is more complex than that assumed in their initial design. The numerical model developed in a separate part II paper[2] throws more light onto the problem.
It is correct to say that the assumptions and simplifications made at design stage did not have a detrimental effect on the static performance of the units. However, as the units behave more like plates (slabs) and less like beams, and if optimum design is to be achieved, it may be useful for the

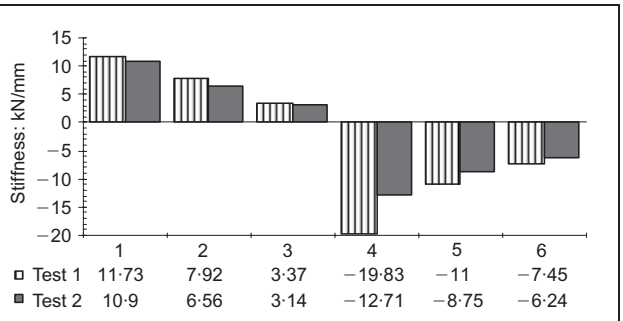

Figure 11. Terrace unit 1, tests 1 and 2, estimated stiffness values, loading–unloading

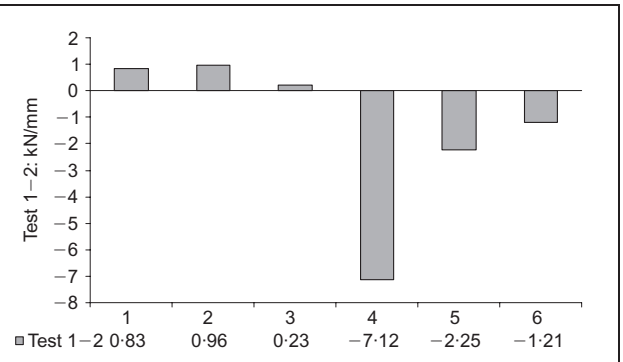

Figure 12. Terrace unit 1, tests 1 and 2, difference between uncracked and cracked local stiffness values, loading–unloading

latter to be approached from a more rigorous angle. The effect of the former on the dynamic performance of the units will be discussed in a different paper.

(*c*) As the corners of the tread tend to turn upwards (warping effect), separating themselves from the propping UB-section and the whole unit bends about two different axis (longitudinal and transverse), a 'trough' forms at the central region of the unit. The above leads to the conclusion that a 'plane of inflexion' (change from concavity to convexity or vice versa) is present. It has not been possible to define the locus of this plane accurately with the information obtained from the laboratory. This is reviewed in the part II paper,[2] given the results from a rigorous finite-element analysis.

(*d*) The maximum displacement of the uncracked unit was found to be higher than the corresponding one for the cracked unit for the same load value. This was because the maximum displacement measured for the cracked unit (test 2) was relative to the residual displacement inherited from test 1, and hence recorded lower. When, however, the permanent displacement from test 1 was added to the corresponding displacement obtained for test 2, the two displacements were found approximately equal, indicating similar irreversible behaviour of the unit before and after cracking.

(*e*) The strain distribution across the depth of the riser was found to be linear and remarkably similar in both tests. The linearity was more evident in test 2, as it is not accompanied by any substantial and sudden change in strain owing to the formation of additional cracks. When the tension zone was developing its first cracks, equilibrium was maintained by a shift of the neutral axis upwards, hence decreasing the sectional area in compression.

(*f*) Strain measured at the longitudinal reinforcement (SG2) is a good indicator of cracks appearing at the tension side of the unit. Strain measured at the lateral reinforcement (SG1) is approximately 21 times smaller than SG2. The 'strain loop' (loading–unloading) for the fully cracked section always enclosed that for the uncracked section.

(*g*) The static stiffnesses of the uncracked unit were found to be greater than that of the cracked unit, as expected, but their difference reduced gradually, with increasing load.

(*h*) The need for more research and reliable modulus of elasticity values for concrete in tension is highlighted.

ACKNOWLEDGEMENTS

The author would like to acknowledge Bison Concrete Products Ltd for its support, and several final-year undergraduate project students for assisting with the tests in the department's laboratories.

REFERENCES

1. DEPARTMENT OF TRANSPORT LOCAL GOVERNMENT AND THE REGIONS, DCMC, INSTITUTION OF STRUCTURAL ENGINEERS. Dynamic performance requirements for permanent grandstands subject to crowd action. In *Interim Guidance on Assessment and Design*. Institution of Structural Engineers, London, 2001.
2. KARADELIS J. N. Concrete grandstands. Part II: numerical modelling. *Proceedings of the Institution of Civil Engineers, Engineering and Computational Mechanics*, 2008, **162**, No 1. 11–21.
3. BRITISH STANDARDS INSTITUTION. *Structural Use of Concrete*. BSI, London, 1997, BS 8110 Part I.